

**Computational Benchmarking and Evaluation of
Transition Metal Complexes toward Materials Discovery**

by

Ryan M. Wheat

B.S. Chemistry, Florida Institute of Technology, 2018

Submitted to the Graduate Faculty of the
Dietrich School of Arts and Sciences in partial fulfillment
of the requirements for the degree of
Master of Science

University of Pittsburgh

2021

UNIVERSITY OF PITTSBURGH

DIETRICH SCHOOL OF ARTS AND SCIENCES

This thesis was presented

by

Ryan M. Wheat

It was defended on

March 30, 2021

and approved by

Geoffrey R. Hutchison, Associate Professor, Department of Chemistry

Kenneth D. Jordan, Distinguished Professor, Department of Chemistry

Peng Liu, Associate Professor, Department of Chemistry

Christopher E. Wilmer, Associate Professor, Department of Chemical/Petroleum Engineering

Thesis Advisor: Geoffrey R. Hutchison, Associate Professor, Department of Chemistry

Thesis Advisor: Kenneth D. Jordan, Distinguished Professor, Department of Chemistry

Copyright © by Ryan M. Wheat

2021

**Computational Benchmarking and Evaluation of
Transition Metal Complexes toward Materials Discovery**

Ryan M. Wheat, M.S.

University of Pittsburgh, 2021

The synergy between computational modeling and materials analysis remains an unsolved problem, yet there is great potential for accelerating materials discovery. This work reframes the cumbersome nature of experimental intuition (trial and error) by shedding light on the utility of quantitative data as a promising alternative. With respect to Metal-Organic Frameworks, stability considerations are essential to the targeting of materials that not only possess high turnover efficiency but are also resistant to degradation. Core computational methods in this work include UFF, GFNFF, GFN2, and B97-3c for their extended utility to evaluating transition metal systems. From a molecular geometry perspective, GFN2 and B97-3c closely matched experimental bond distances for a selected series of 32 transition metal complexes (TMCs) labeled TMC32. In terms of electronic energy, bond dissociation was targeted as a means of predicting synthetic tractability and expected stability. From a separate set of 30 TMCs labeled TM30, B97-3c single-point calculations with UFF optimized geometries provided the highest accuracy. A subset of the tmQM dataset, focused solely on complexes with Ni-Cl bonds, supported the argument that GFN2 is infeasible for calculating electronic effects in its current state. These studies elevate B97-3c as an efficient method that can accelerate efforts to quantify stability in TMCs, with future work focused on correlating this data to improve MOF modeling capabilities towards materials discovery.

Table of Contents

1.0 Introduction	1
1.1 Historical Relevance	2
1.2 Metal-Organic Frameworks	3
1.3 Thermal and Chemical Stability	5
1.4 Force Field Optimization	7
1.5 Approximate Density Functional Theory Methods	8
2.0 Dataset Selection and Software	10
3.0 Computational Results	11
3.1 Bond Enthalpy Calculations	11
3.2 Bond Distance Analysis	14
3.3 Bond Stretch Behavior	15
3.4 Bond Order Analysis	18
4.0 Conclusions	20
Appendix A Geometric Depictions of $\text{Ti}(\eta^5\text{-C}_5\text{H}_5)_2(\text{Cl})_2$ and TiO_2	21
Bibliography	22

List of Figures

Figure 1 Side-by-side Comparison of MOF-5/IRMOF-1 Unit Cell.....	4
Figure 2 Mean Deviations of BDE from Experimental Values 1.....	11
Figure 3 Mean Deviations of BDE from Experimental Values 2.....	12
Figure 4 Statistical Analysis for BDE Deviations from Experimental Values	12
Figure 5 Bond Distance Analysis from TMC32 Dataset	14
Figure 6 Bond Order vs. Mn-C₅H₅ Bond Deviation (Mn(η^5-C₅H₅)(CO)₃)	16
Figure 7 Bond Order vs. Co-NO Bond Deviation (Co(CO)₃(NO)).....	16
Figure 8 Bond Order vs. Cu-CN Bond Deviation (CuCN)	17
Figure 9 Dependence of Bond Order on Bond Distance for Ni-Cl Complexes	18
Figure 10 Correlation Plot between B97-3c and GFN2 for Ni-Cl Complexes.....	19
Appendix Figure 1 GFN2 Depictions of Ti(η^5-C₅H₅)₂(Cl)₂ (Left) and TiO₂ (Right).....	21
Appendix Figure 2 B97-3c Depictions of Ti(η^5-C₅H₅)₂(Cl)₂ (Left) and TiO₂ (Right)	21

1.0 Introduction

Reliance on non-renewable energy has led to catastrophic environmental impacts, among the most damaging arising from global warming and increases to pollution. This precipice of human-made destruction can potentially bring about societal collapse, with economic demand bleeding into the already tensioned political ecosystem. Despite the incorporation of non-toxic chemical substitutes in manufacturing and introduction of efforts to recycle components, the overwhelming reliance on non-renewable energy and its corresponding waste products remains unsolved. To address this issue, means of isolating/storing volatile organic compounds (VOCs) and replacing the burning of fossil fuels would significantly help mitigate the environmental impacts of these VOCs. Metal-Organic Frameworks (MOFs) provide a means to capture and sequester VOCs both reversibly and efficiently. Sensitivity to environmental conditions and resistance to degradation are two important factors in enhancing utility.

Computational modeling would provide a means to analyze the reactivity, selectivity, and properties of MOFs. However, evaluating the electronic structure of a MOF requires high levels of theory attune to that of Density Functional Theory (DFT), perturbation theory, and coupled cluster methods, which are intractable for large-scale benchmarking^{1,2,3}. Limitations in generalizing the binding modes, intramolecular forces, and electrostatics over an extended area yields substantial systematic error. Considering that the bulk of inorganic materials rely on reactivity and structural selectivity at or near the metal ion, large-scale analyses of transition metal systems could provide insight to the properties of larger materials. This work attempts to leverage method accuracy with computational cost as its primary goal, relying on statistical analysis to generalize trends for transition metal complexes toward improving future MOF modeling.

1.1 Historical Relevance

Transition metals continue to see persistent utility in sustainable materials engineering, a field blossomed from incentivizing the combat of persistent, non-sustainable pollutants. These transition metal complexes are not a new technology, with considerable interest in coordination complexes dating to the discovery of dye substances used by ancient Egyptians. Among such compounds is bright alizarin red, a hydroxyanthraquinone complex chelated to calcium and aluminum. A more recent example is the substance Prussian blue ($\text{KFe}_4^{\text{III}}[\text{Fe}^{\text{II}}(\text{CN})_6]_3$), used as a paint pigment since the dawn of the 18th century during the Baroque period. Debates regarding the underlying structure of these colorful compounds intrigued scientists, with Christian Blømstrand and Sophus Jorgensen's chain theory being the most widely accepted. Alfred Werner challenged this theory with ideas of a coordination sphere and spatial ligand arrangements, awarding him the 1913 Nobel Prize in Chemistry. This 'standard model' sheds light on additional aspects for these complexes, such as rigidity, hydrophilicity, and crystallinity, all of which crucial to this work.

Stability from a transition metal standpoint is considered by the extent of orbital overlap. The strengthened binding between transition metals contributes to their materials properties. Whereas hardness and resistance to degradation contributes to stability, the ease of electron mobility elevates these metals to new heights, allowing for the invention of wiring, telephones, and computer devices. Nowadays, transition metals such as chromium, platinum, and gold are commonplace for applications such as chrome plating, catalytic converters, and even jewelry, among others. Combinations of transition metals yield synergistic materials with enhanced utility. Furthermore, we can take advantage of transition metal rigidity and electron mobility while also introducing organic ligands to improve flexibility, yielding superior metal-organic based structures with adaptable materials applications.

1.2 Metal-Organic Frameworks

The versatility of possible bonding schemes enhances the appeal of metal complexes for usage in applications such as water treatment and ceramics^{4,5}. The recently popularized Metal-Organic Frameworks (MOFs) lie at the junction between solid state chemistry and engineering^{6,7,8}. Considerable attention has been drawn to this area of research due to the ease with which rational design and high throughput synthesis are capable thanks to the aforementioned transition metal complexes as building blocks. Weakly coordinating solvents prepare a template/skeleton for MOF crystallization in solution, with conditions such as pressure, humidity, temperature, pH, concentration, and reagent stoichiometry affecting the final structure^{9,10}. This incredible selectivity is not isolated to MOFs, but as a result, this reduces the design, synthesis, and planning of new adsorption-based technologies for gas storage, catalysis, and solar harvesting applications¹¹.

Despite the vast potential that MOFs can theoretically achieve, there is a caveat: synthetic intuition (trial & error) remains essential for synthetic design of new MOF species. Nonetheless, traditional ligand field theory provides insight on the ligand exchange rates, and while stoichiometric quantities of reagents can be a good first estimate, most systems do not exactly abide by this logic. Furthermore, design of multicomponent MOF structures relies on solutions containing multiple inorganic and/or organic counterparts, which can be extremely challenging to plan without prior experience. There is, however, some sense of restriction as crystalline MOFs have a known limited number of possible mathematical morphologies (topologies) that can provide blueprints for growing MOFs in solution. Yet, considering the prevalence of isorecticular studies, these variants do not necessarily follow the same synthetic conditions or morphology, further inhibiting chemical intuition as there are no direct logical correlations between either mechanism.

In practice, this bottleneck emerges from poor understanding of the reorganization of transition metal nodes into symmetrically placed secondary building units (SBUs), connected by extensions of organic ligands (linkers) that help dictate pore size and chemical reactivity. A computational perspective would reframe synthesis from a ground-up perspective, instead relying on quantitative values rather than synthetic intuition. With the MOF field in its infancy, this work focuses on the critical understanding of the tougher-to-calculate inorganic moieties and their properties, such as bond order, spatial arrangement of ligands, and energies. This, in turn, will help to better define thermal and chemical stability as a foundation for accelerating MOF discovery. As a supplement for understanding MOFs, **Figure 1** shown below illustrates the skeleton (left) and space-filling (right) model of IRMOF-1, otherwise known as MOF-5. The void space in the center of the structure is where chemical or physical adsorption can occur. High surface area increases the loading efficiency with which selective uptake of molecules (i.e., VOCs) can be performed.

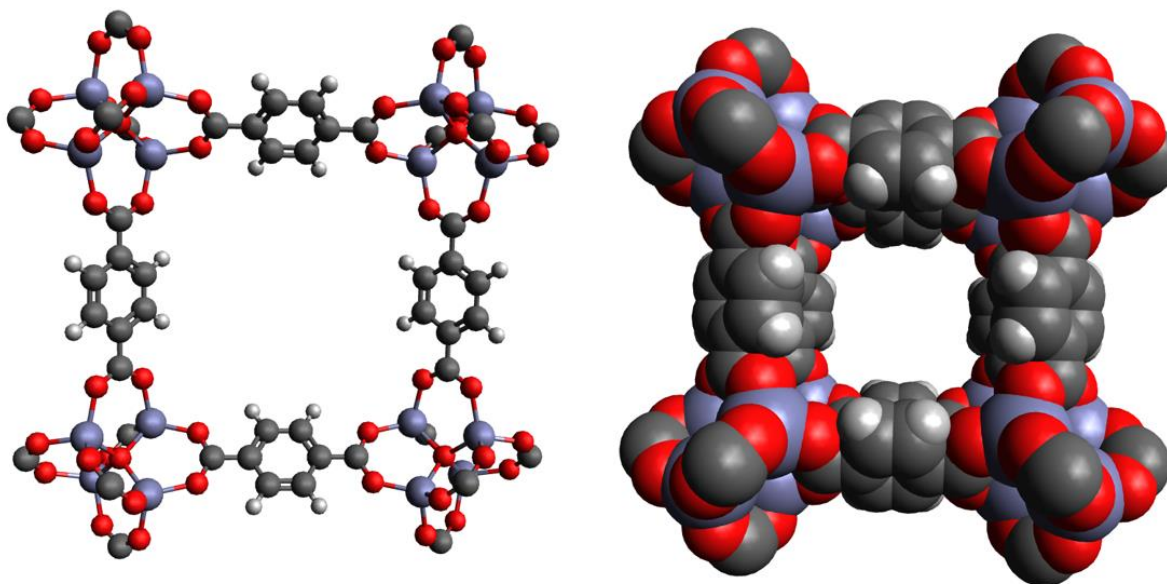


Figure 1 Side-by-side Comparison of MOF-5/IRMOF-1 Unit Cell

1.3 Thermal and Chemical Stability

In the context of this work, “stability” refers to the set of environmental parameters or conditions in which a material resists degradation over a defined duration¹². For MOFs, exposure time is based on both chemical and thermal factors, typically correlated to the reaction conditions from which the MOF was synthesized. Additionally, crystallinity heavily contributes to stability as tightly packed systems are resistant to chemical attacks. Yet, pore size is inversely proportional to interpenetration, contributing to an overall loss in applicability. Thus, an ideal MOF would synergistically combine exposure resistance to various conditions and also large macropore void-space for adsorbates to bind, either for storage or chemical conversion. This sensitive equilibrium is crucial, yet it is an unsolved problem for reticular chemists from a quantitative standpoint. However, there are various known qualitative factors that affect stability.

MOF applications may require some form of solvent exchange within adsorbable pores or exposure to non-inert conditions. Low valent transition metals, such as Zn^{2+} , are susceptible to aqua ligand exchange leading to hydrolysis. Higher valence metals, like Cr^{3+} , have enhanced stability from high steric hindrance, reducing ligand competition. In this way, highly charged transition metals form a ligand shield around themselves, both enhancing structural rigidity while also reinforcing chemical stability. Chemically stable MOFs are sometimes synthesized under acidic conditions with modulators, reducing the presence of metal-oxide or metal-hydroxide side products¹³. Substituting carboxylic end groups with imidazole and incorporating alkyl alcohols during synthesis have shown to strengthen metal-ligand bonds and increase hydrophobicity, respectively^{14,15}. Modifying the organic linker to a polycarboxylic variant provides more structural stability stemming from additional connectivity¹⁶, but modification of the underlying crystal structure through alterations is possible.

From a thermodynamic perspective, increasing energy to the system affects degradation in several stages. Heating drives off residual solvent locked in pores, then as temperature increases, solvated molecules coordinated to the metal node are removed, leading to open metal sites that are susceptible to chemical attack. Linkers are last to dissociate yielding degradation of the framework, as bond enthalpy between metals and polydentate ligands surpasses solvent coordination. These effects are correlated to chemical stability, as MOF susceptibility to degradation accelerates even in relatively inert atmospheric conditions from oxidation. In a closed system, the ligand exchange rates are amplified by dissociated solvent molecules rebinding to open metal sites.

The MOF free energy is heavily dependent on crystal packing and topology, although solid defects are prime candidates for cascading degradation. Shear planes between unit cells present a synthetic challenge, as this reduces structural integrity. Deformation or reorganization of the metal-organic framework occurs simultaneously with molecular / structural changes, eventually yielding metal-organic powder at a temperature threshold. Many of the rules in chemical stability apply to thermal stability as well. Stable, highly valent oxidation state subunits with greater degrees of nuclearity are favorable over discrete building units. One exception is infinite rod building units, like that of MOF-74, which possess impressive stability in inert, heated conditions even with divalent cations¹⁷. Such discoveries are pivotal for expanding avenues for applications.

Considering the depth with which MOF stability is based, quantitative studies would have a pronounced effect on improving MOF modeling from a computational standpoint. Such a feat is intractable for a single body of work, and as such the goal is to evaluate the suitability of modern computational methods for analyzing geometries and energies for transition metal complexes, as this would provide a means to consider large-scale benchmarking of complexes. In turn, this would yield a vast set of quantitative data to provide context for MOF stability.

1.4 Force Field Optimization

With respect to transition metal complexes, force-field optimization persistently is the most tractable form of computation available. At the classical level of theory, force-field codes such as UFF approximate the electronic energy with fitted parameters and molecular descriptors such as bond order, electrostatic forces, and atomic charges¹⁸. This significantly accelerates calculations.

Harmonic and Morse oscillator approximations are essential for calculating bonding energies, and force constant selection contributes to the evaluation of molecular geometry. The bonding and nonbonding energy terms intend to capture point-charge electrostatics, van der Waals forces, and inversion characteristics. Overall, this approach maintains a classical perspective by only considering elemental composition, connectivity, and hybridization in parameter evaluation.

Extending the scope of what is captured in the electronic energy can be achieved one of two ways: (1) introducing new terms to the energy expression or (2) updating parameters and force-constants to capture a wider set of structures. Both are accounted for with Grimme's recent GFN force-field (GFN-FF)¹⁹. Introduced here are updated charge models, parameters fitted to a B97-3c functional, extended non-covalent binding schemes, and three-body bond corrections. Electrostatics are accounted for with an electronegativity equilibration model. Changing from a point-charge method (UFF) to one based on variationally treated charge density fluctuations gives a refined electrostatic picture, thus making this force-field (GFN-FF) partially polarizable. Additionally, GFN-FF gives explicit focus to both hydrogen-bonding (E_{HB}) and halogen-bonding (E_{XB}), included to capture dipole-dipole interactions. All of these factors would be advantageous for modeling inorganic complexes, as the properties of the central transition metal persistently and dynamically change to accommodate ligand exchange rearrangements in solution.

1.5 Approximate Density Functional Theory Methods

As a preface to this section, we consider here the tight binding approximation to Density Functional Theory (DFTB)²⁰. An orbital representation is variationally derived and then used to make linear combinations, forming Kohn-Sham (KS) orbitals. This replaces the tedious derivation of calculating the Hamiltonian and overlap matrices, but is itself non-self-consistent, representing only a zeroth order solution. Instead, core electrons are frozen in favor of only considering density fluctuations around the valence space. The Hamiltonian is broken into approximate electrostatic, exchange-correlation, and dispersion terms, requiring the calculation of parameter free gradients, integrals, and a variational algorithm to retrieve a minimum energy solution.

By comparison, the recently developed semi-empirical tight binding GFNn-xTB²¹ prepared by Grimme's group accelerates this approach by reintroducing fitted parameters alongside an iterative extended-Hückel calculation. Three variations exist for GFNn-xTB methods: GFN0, GFN1, and GFN2. Numerical increments correlate with enhanced electronic accuracy, with GFN2 performing better than GFN1 and GFN0. This work focuses solely on GFN2, a method that inherently relies on element-specific parameters for evaluating monopole, dipole, and quadrupole. Multipole moments are then utilized to approximate both isotropic and anisotropic effects. GFN2 incorporates the D4 dispersion correction scheme, featuring both a three-body correction and Becke-Johnson (BJ) damping, to enhance long-range intermolecular effects, pivotal for non-covalent interactions²². Cumulative atomic dipole and traceless quadrupole moments define anisotropy, included to extend the intermolecular nonbonding regime through enhanced descriptions of electronic density fluctuations around weakly coordinating elements. These factors make GFN2 an attractive method for analyzing transition metal systems by enhancing descriptions of bonding and non-bonding interactions for ground state geometries.

Despite success with tight-binding DFT, no corrections to the electron correlation term are included, essentially ignoring spin polarization. In this work, Becke's 1997 (B97) generalized gradient approximation (GGA) functional is used with Grimme's D3 dispersion correction scheme and an Axilrod-Teller-Muto (ATM) three-body term, referred to as B97-3c²³. This revised functional incorporates semi-empirical parameterization and removal of Fock exchange to accelerate calculations. The density dependent exchange-correlation functional is formally based on the uniform electron gas (UEG) model to derive local energy densities, with correction factors implemented to achieve a balance between flexibility and generality without over-fitting. Finally, a modified diffuse basis set (def2-mTZVP) consists of edits to polarization parameters for lighter elements (H-Ar) to improve intermolecular force descriptions and reduce computational time. Justification for this method is given by low mean deviations in metal-ligand bond lengths and bond dissociation enthalpies for transition metal complexes compared to experimental results²⁴.

2.0 Dataset Selection and Software

In benchmarking energies for transition metal complexes (TMCs), this work will use Becke and Johnson's 2009 study as a basis for comparing the above-mentioned methods to experimental results²⁵. Bond dissociation enthalpy calculations are reported for a series of 30 neutral close shell 3d transition metal complexes with small- to moderate- sized ligands which will be labelled TM30. Accurate descriptions of bond geometry are tested with the TMC32 dataset, motivated from a similar study by Grimme's group that gave promising results for both B97-3c and GFN2. Both datasets are similar in construction, although relatively small in size. As such, this work also includes a nickel subset of the tmQM dataset, which comprises some 86,000 complexes borrowing from structures reported in the Cambridge Structural Database (CSD)²⁶. For GFN2 and GFN-FF, version 6.3.0 of the xTB program was used. Separately, GFN2 version 6.1.4 was used in the original publication of the tmQM dataset. Avogadro version 1.2.0 was used to perform UFF optimizations on the TMCs using OpenBabel version 2.3.0^{27,28}. Also, ORCA version 4.0.2 was used to perform DFT calculations with the B97-3c functional^{29,30}.

3.0 Computational Results

3.1 Bond Enthalpy Calculations

Enthalpies are reported as an average over the number of ligands per complex, with fragments assessed as radicals. Methods with the slash “/” nomenclature refers to geometry optimizations with the first method and single-point evaluations with the second (i.e., GFNFF / B97-3c → GFNFF geometry optimization followed by B97-3c single-point calculation). Both **Figures 2** and **3** illustrate how well each computational method compared to experimental gas-phase findings. The bar graph is separated by transition metal, with data coming from an average over all respective complexes. Both mean absolute deviation and standard deviation are shown in **Figure 4** for all six methods.

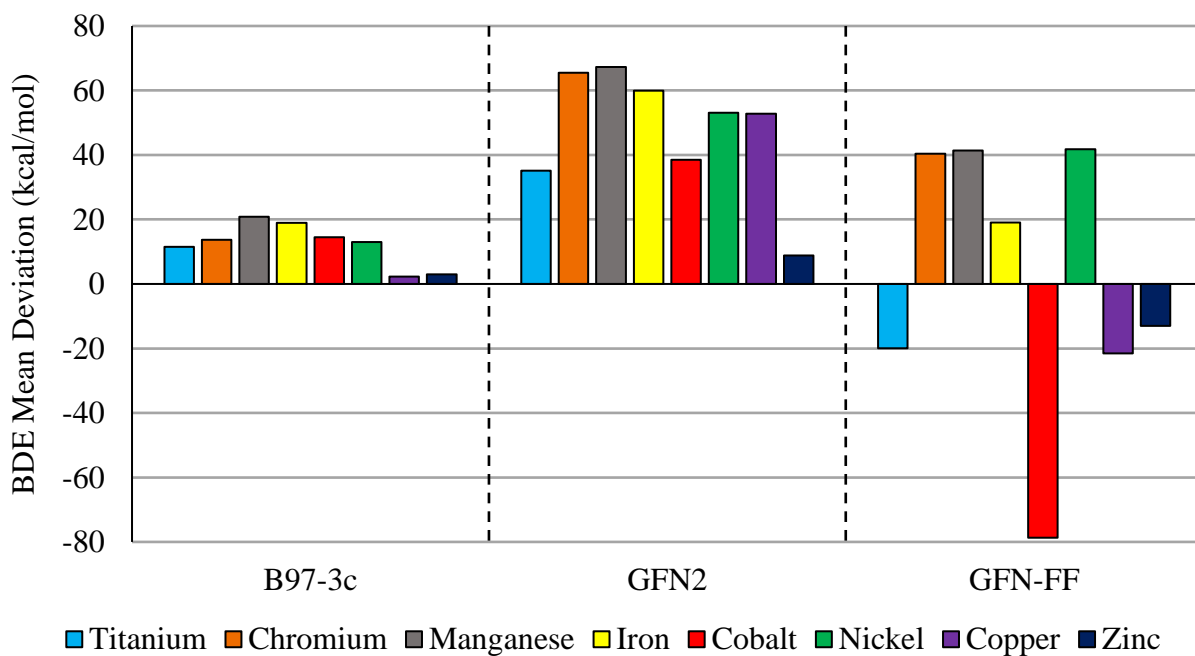


Figure 2 Mean Deviations of BDE from Experimental Values 1

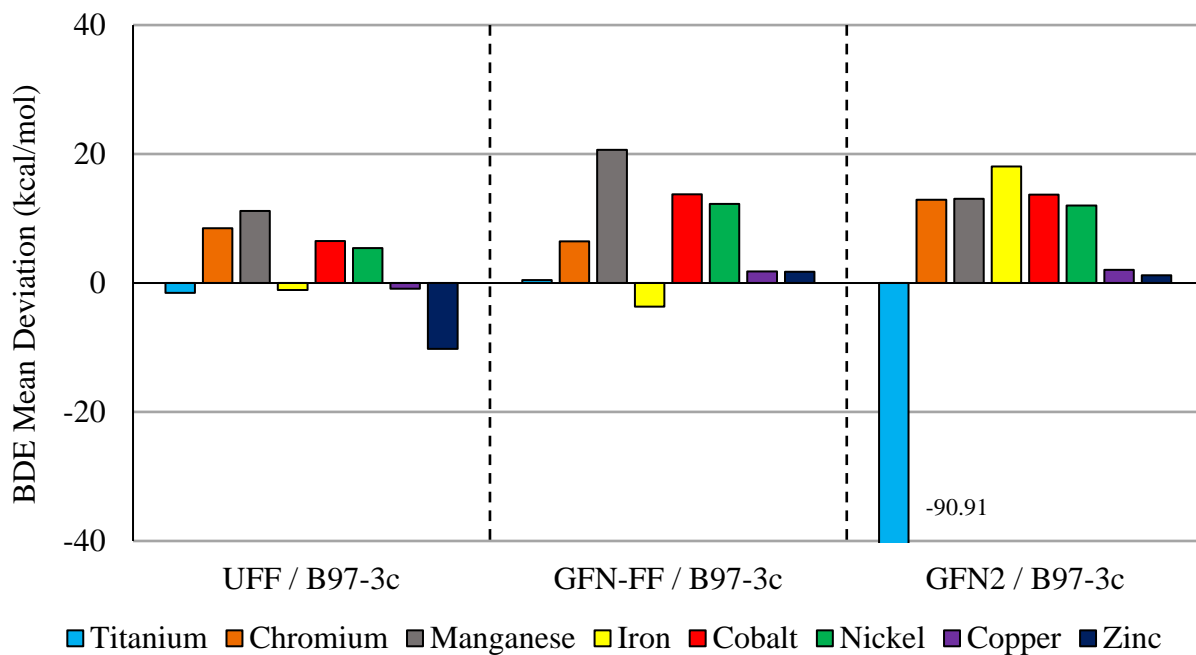


Figure 3 Mean Deviations of BDE from Experimental Values 2

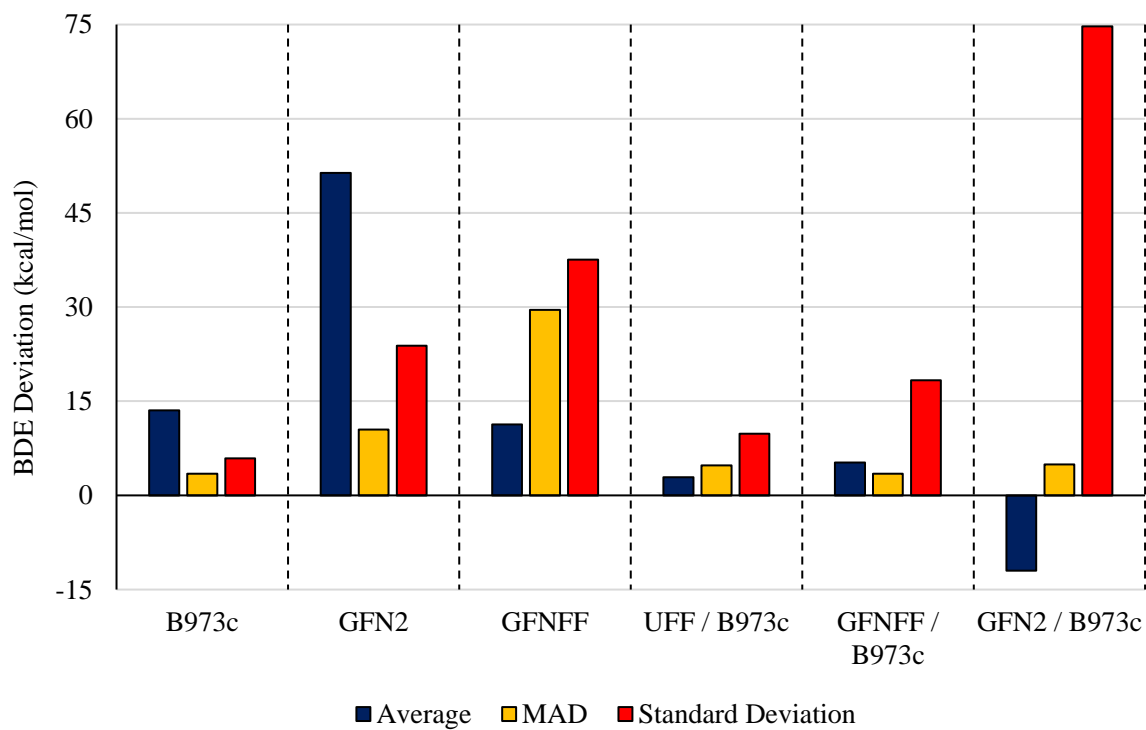


Figure 4 Statistical Analysis for BDE Deviations from Experimental Values

The classically based analysis of complexes from TM30 with force-field optimized geometries were sufficient as a first approximation, driving down deviated errors with the B97-3c single point calculations as shown in **Figure 3**. Yet, B97-3c is necessary to extract accurate energies, illustrated in **Figure 2** by the higher deviation in BDE for GFN2 and GFNFF when compared to B97-3c calculations. The significant standard deviation for GFN2/B97-3c in **Figure 4** can be attributed to two particular complexes: $\text{Ti}(\eta^5\text{-C}_5\text{H}_5)_2(\text{Cl})_2$ and TiO_2 (**Appendix A**). Excluding these two complexes, the standard deviation decreases to 14.94 kcal/mol. An unprecedented result, the accuracy of the B97-3c functional for calculating BDE is sensitive to geometry distortions from equilibrium, with UFF and GFNFF providing good representations.

Parameterization typically restricts at least some generality, as over-fitting leads to non-transferability for analyzing diverse datasets. Both GFN2 and GFN-FF methods are curated to accommodate a variety of broad applications, yet focus was shifted away from dissociation enthalpies, instead emphasized on ground-state geometries. GFN2 is more predictable in that all transition metals in **Figure 2** having positive mean deviations. GFN-FF meanwhile is sporadic by comparison, a logical conclusion given that explicit isotropic and anisotropic polarizabilities in GFN2 enhance descriptions of electron diffusivity in these complexes.

3.2 Bond Distance Analysis

Initial findings with B97-3c and GFN2 show accurately approximated metal-ligand bond lengths for 32 transition metal complexes. With the same TMC32 dataset, both UFF and GFNFF are assessed. Results in **Figure 5** illustrate the average, mean deviation, and standard deviation with respect to experimentally found bond lengths, derived from corresponding crystal structures. In total, 50 bond lengths make up the dataset, with some complexes having been repeated to assess different ligands. For example, the complex $\text{Fe}(\eta^5\text{-C}_5\text{H}_5)(\text{CO})_3$ is presented twice, once as a Fe-CO bond and another time as Fe-C₅H₅.

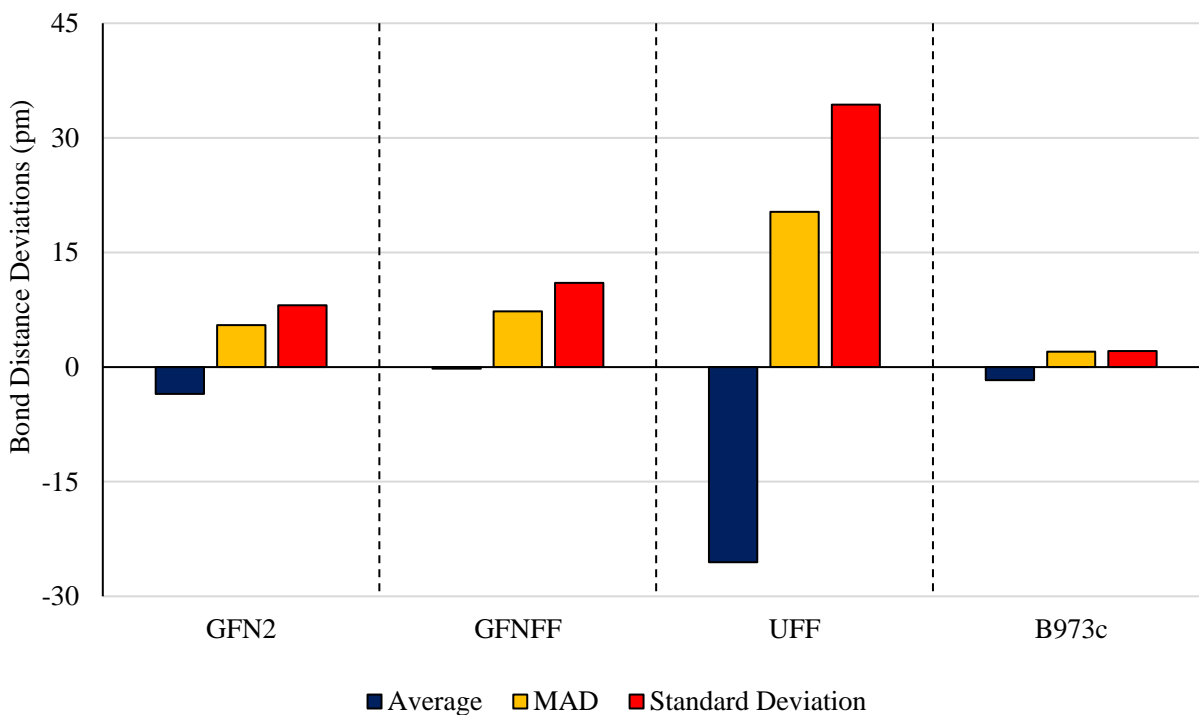


Figure 5 Bond Distance Analysis from TMC32 Dataset

The results in **Figure 5** contradict the bond enthalpies in **Figure 3**, with UFF and GFNFF providing trial structures that, despite being inaccurate, produced accurate bond enthalpies with B97-3c single-point calculations. Theoretically, accurate geometries and energies are correlated, with higher levels of theory providing more accurate results. It is clear that force-field methods provide poor molecular geometries, given that they miss on crucial non-covalent interactions that methods like GFN2 and B97-3c incorporate explicitly. Yet, the extent of parameterization for force-field methods provides a much-needed tradeoff, mitigating computational resources at the cost of accuracy. The B97-3c functional appears to overbind bonding interactions, observed from the 10-20 kcal/mol deviation in enthalpy upon optimizing geometries (**Figure 2**). Yet, force-field methods tend to undermine bonding, balancing out B97-3c when used as a single-point method, indirectly increasing accuracy for this specific dataset. The worse performance of both GFN2 and GFN-FF variants with B97-3c single point rests on the accuracy with which bond distances are assessed, ultimately increasing the bond enthalpy deviations as a result. This further supports the “averaging out” hypothesis, given that the poor performance of UFF for bond distances would shift the enthalpy deviation down, in this case getting closer to experimental values.

3.3 Bond Stretch Behavior

Unrelaxed bond distance scans were completed for complexes in the TMC32 dataset, with **Figures 6, 7, and 8** shown to illustrate the relationship between bond order and distance for both GFN2 and B97-3c methods. Starting structures were derived from B97-3c geometry optimization. These complexes were selected to because of their well-known bonding arrangements as well as the features present in the following plots.

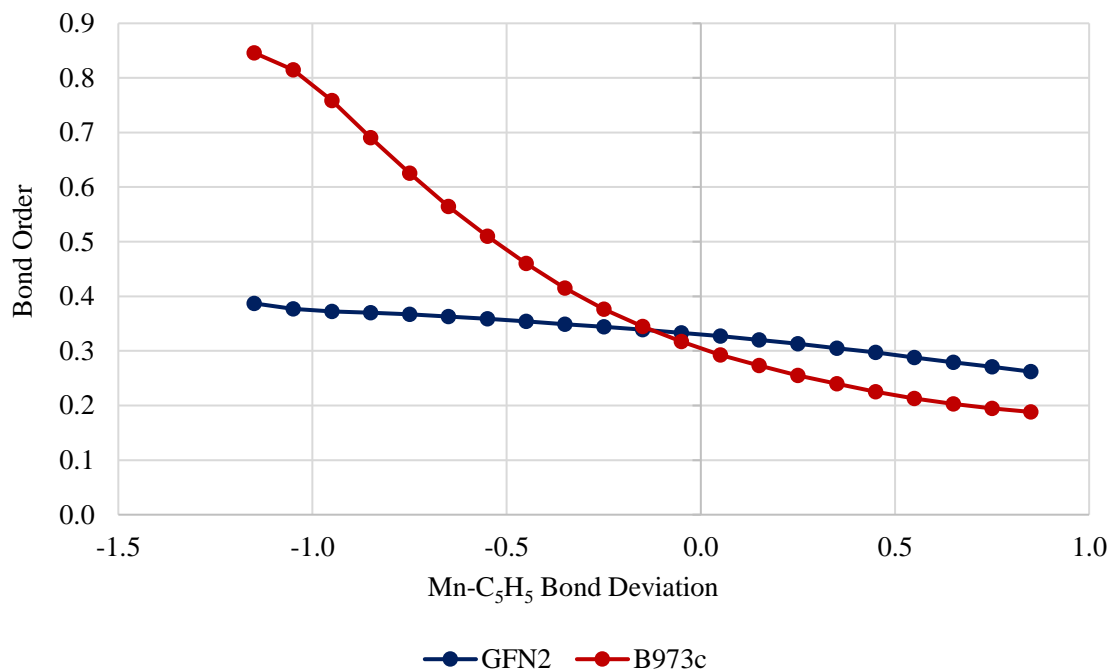


Figure 6 Bond Order vs. Mn-C₅H₅ Bond Deviation (Mn(η⁵-C₅H₅)(CO)₃)

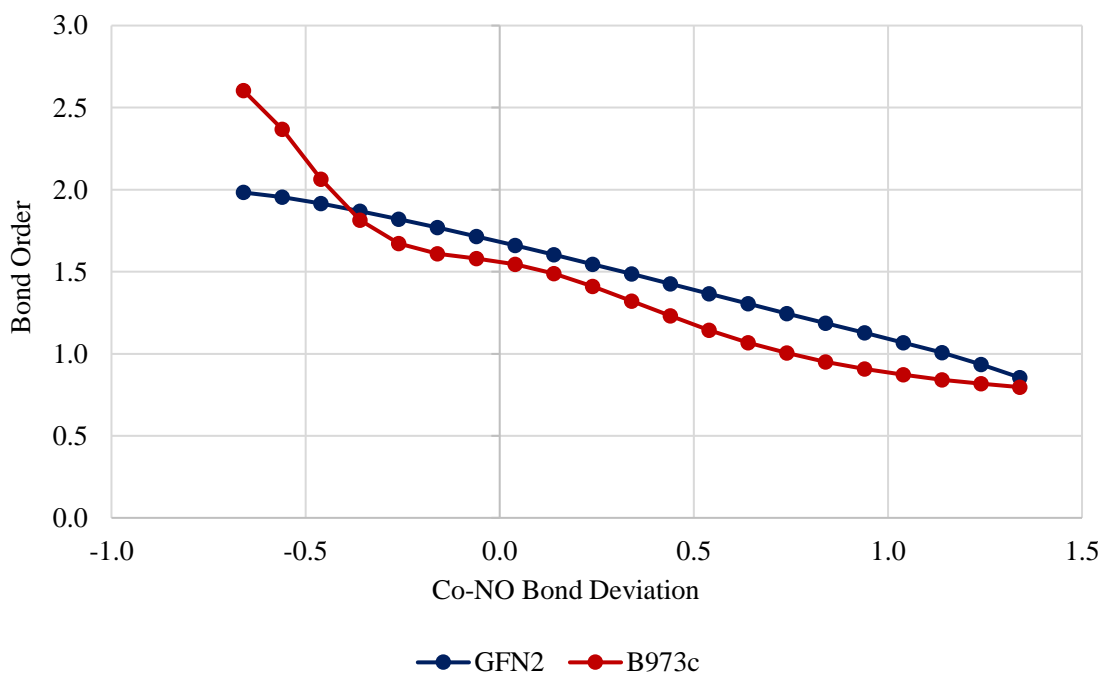


Figure 7 Bond Order vs. Co-NO Bond Deviation (Co(CO)₃(NO))

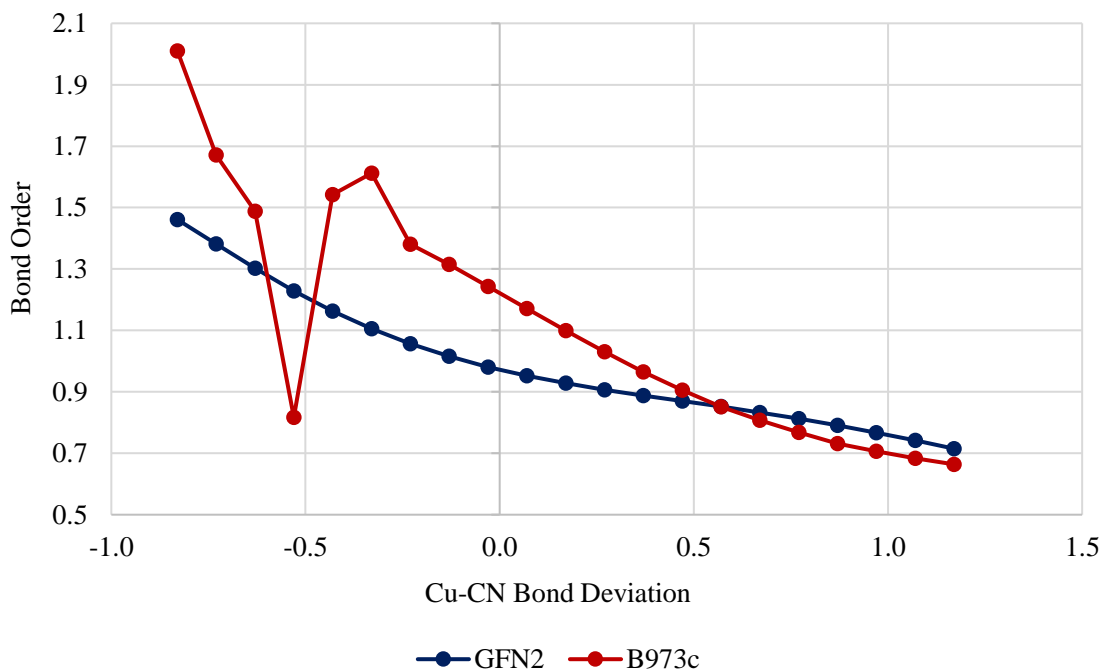


Figure 8 Bond Order vs. Cu-CN Bond Deviation (CuCN)

Within the context of this work, bond order is defined as the probability density resulting from orbital overlap. As illustrated in **Figures 6 and 7** the GFN2 curve is nearly flat, whereas in **Figure 8** the plot is approaching a power-series relationship. This reveals the insensitivity with which GFN2 has compared to B97-3c. Considering that non-covalent interactions were a critical concern in developing GFN2, this result is unexpected. On the other hand, B97-3c bond-dissociation curves can produce unanticipated results due to bond shrinking in the repulsive regime (**Figure 8**). This is unusual given that bond distance scans were unrelaxed (not optimized), hence bond geometry would not change. Considering the Cu-N bond order increase alongside the decrease with Cu-C, perhaps ORCA is anticipating a geometry rearrangement.

3.4 Bond Order Analysis

To further illustrate the bond length discrepancy, both GFN2 and B97-3c were evaluated for 462 Nickel complexes from the tmQM dataset. These complexes feature Chloride ligands that have a relatively high calculated bond order with Nickel compared to other ligands.

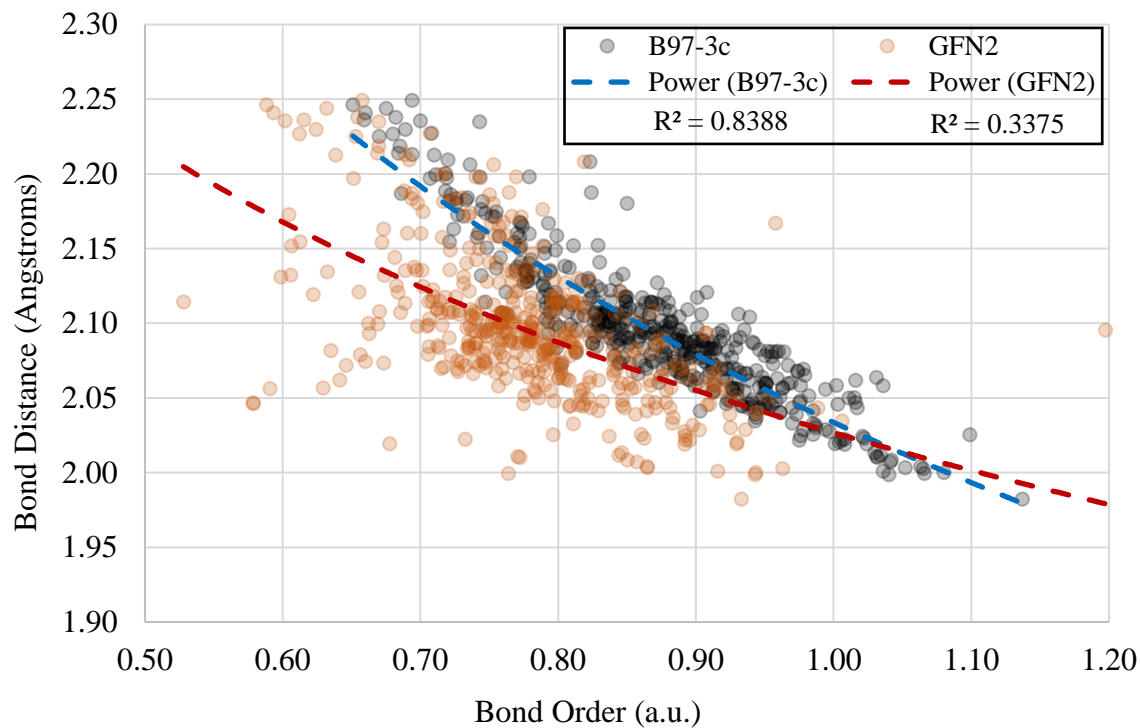


Figure 9 Dependence of Bond Order on Bond Distance for Ni-Cl Complexes

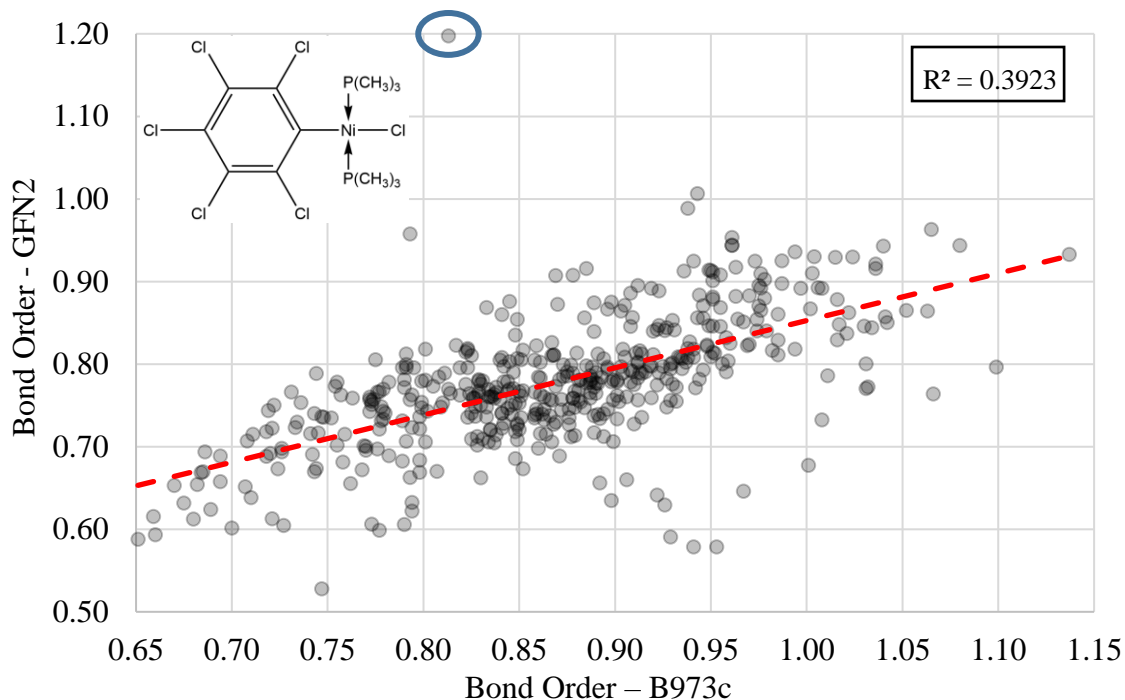


Figure 10 Correlation Plot between B97-3c and GFN2 for Ni-Cl Complexes

This Ni-Cl subset was selected because of the prevalence of this bond type in the dataset and the limited bonding modes for these complexes. Based on the r^2 values in **Figures 9** and **10**, bond lengths are better correlated to bond order with B97-3c rather than GFN2. This reflects the poor performance of GFN2 towards calculating electron density, which not only affects bond order but also multipole moments and electronic energies. **Figure 2** support this argument given the overestimation of bond enthalpies for GFN2. The complex shown in **Figure 10** (circled) is a significant outlier for the correlation plot between both GFN2 and B97-3c methods. Removing this complex improves the calculated r^2 to 0.4293. Given the bonding underestimation for C_5H_5 ligands in GFN2, it is expected that chloride would have a higher bond order to compensate.

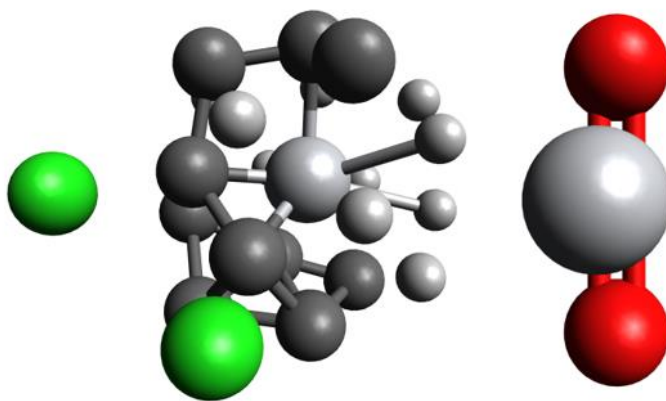
4.0 Conclusions

The restricted utility of qualitatively based synthetic intuition toward the design of new materials remains a bottleneck for research and development. In the context of MOFs, long term stability from a chemical and thermal standpoint are crucial when targeting industrial applications. Computational modeling holds promise toward evaluating ideal environmental and synthetic conditions, although the inefficiency of modern methods for calculating large framework systems remains an issue. Instead, the presented computational approach postulates the utility of modeling MOF components, specifically transition metal systems, as a means to approach the study of stability from a quantitative standpoint.

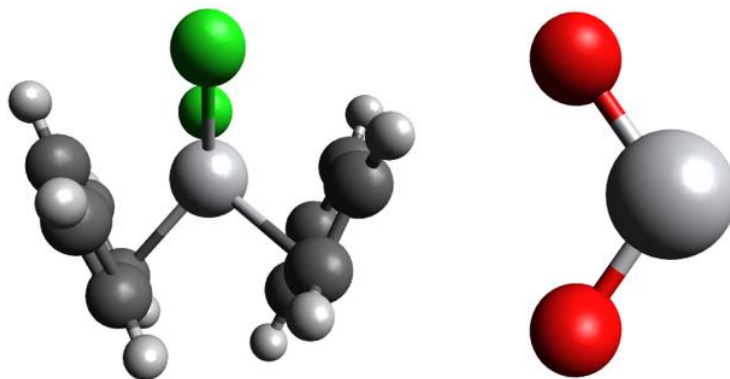
Tabulated results illustrate the potential with which B97-3c and GFN2 have for analysis of transition metal complexes. GFN2 is a reasonable method for evaluating molecular geometries at the ground state in some respects, but the sporadic bond order results shown in **Figure 9** and the weak correlation to B97-3c given in **Figure 10** are troublesome, hindering this method from accurately analyzing stability factors for mechanistic analyses. Considering that MOF formation hinges on solvent/ligand exchange, bond stretching and shrinking are important factors, yet GFN2 is insensitive in both regimes when compared to B97-3c. An unanticipated side effect, geometry optimization with UFF followed by B97-3c single-point calculations provide more accurate enthalpies than optimization with B97-3c alone. The potential for UFF/B97-3c as outlined requires more benchmarking validation including the tmQM dataset. Additional work could target the efficacy of improving GFN2 by means of updated parameters focused on MOF components, especially for systems where transition metals are binding to aromatic ligands.

Appendix A Geometric Depictions of $\text{Ti}(\eta^5\text{-C}_5\text{H}_5)_2(\text{Cl})_2$ and TiO_2

Two complexes from the TM30 dataset significantly increased the mean enthalpic deviation for the GFN2/B97-3c method when compared to experimental values, as depicted in **Figure 3**: $\text{Ti}(\eta^5\text{-C}_5\text{H}_5)_2(\text{Cl})_2$ and TiO_2 . This deviation is attributed to poor geometry optimizations of structures at the GFN2 level, as shown below in **Appendix Figure 1** when compared to structures optimized with the B97-3c method, given in **Appendix Figure 2**.



Appendix Figure 1 GFN2 Depictions of $\text{Ti}(\eta^5\text{-C}_5\text{H}_5)_2(\text{Cl})_2$ (Left) and TiO_2 (Right)



Appendix Figure 2 B97-3c Depictions of $\text{Ti}(\eta^5\text{-C}_5\text{H}_5)_2(\text{Cl})_2$ (Left) and TiO_2 (Right)

Bibliography

- [1] Yang, Q.; Liu, D.; Zhong, C.; Li J. R. *Chem. Rev.* 2013, 113, 8261-8323.
- [2] Grajciar, L.; Bludsky, O.; Nachtigall, P. J. *Phys. Chem. Lett.* 2010, 1, 3354-3359.
- [3] Grajciar, L.; Nachtigall, P.; Bludsky, O.; Rubes, M. J. *Chem. Theory Comput.* 2015, 11, 230-238.
- [4] Pohl, A. *Water Air Soil Pollut* 2020, 231, 503.
- [5] Kothiyal, G.P. et al. *J Adv Ceram* 2012, 1, 110–129.
- [6] Bureekaew, S.; Shimomura, S.; Kitagawa S. *Sci. Technol. Adv. Mater.* 2008, 9, 014108.
- [7] Furukawa, H.; Cordova, K. E.; O’Keeffe, M.; Yaghi, O. M. *Science* 2013, 341, 1230444.
- [8] O’Keeffe, M. and Yaghi, O. M. *Chem. Rev.* 2012, 112, 675-702.
- [9] Ferey, G. *Chem. Soc. Rev.* 2008, 37, 191-214.
- [10] Li, N. et al. *Chem. Commun.* 2016, 52, 8501-8513.
- [11] Kumar, P. et al. *Microporous and Mesoporous Materials* 2017, 253, 251-265.
- [12] Mouchaham, G.; Wang, S.; Serre, C. *The Stability of Metal-Organic Frameworks. Metal Organic Frameworks: Applications in Separations and Catalysis*, 1; Hermenegildo, G. and Navalón, S., Eds.; Wiley-VCH Verlag GmbH & Co. KGaA, Boschstr.: Weinheim, Germany, 2018; 1–28.
- [13] Schaate, A. et al. *Chem. Eur. J.* 2011, 17, 6643–6651.
- [14] Eddaoudi, M. et al. *Chem. Soc. Rev.* 2015, 44, 228–249.
- [15] Yang, J.; Grzech, A.; Mulder, F.M.; Dingemans, T.J. *Chem. Commun.* 2011, 47, 5244-5246.
- [16] Low, J.J. et al. *J. Am. Chem. Soc.* 2009, 131, 15834–15842.
- [17] Rosi, N.L. et al. *J. Am. Chem. Soc.* 2005, 127, 1504–1518.
- [18] Rappe, A. K. et al. *J. Am. Chem. Soc.* 1992, 114, 10024-10035.
- [19] Spicher, S. and Grimme, S. *Angew. Chem.* 2020, 132, 2-11.
- [20] Seifert, G. J. *Phys. Chem. A* 2007, 111, 5609-5613.

- [21] Bannwarth, C.; Ehlert, S.; Grimme, S. *J. Chem. Theory. Comput.* 2019, 15, 1652-1671.
- [22] Caldeweyher, E. et al. *J. Chem. Phys.* 2019, 150, 154122.
- [23] Brandenburg, J. G.; Bannwarth, C.; Hansen, A.; Grimme, S. *J. Chem. Phys.* 2018, 148, 064104.
- [24] Hughes, T. F.; Harvey, J. N.; Friesner, R. A. *Phys. Chem. Chem. Phys.* 2012, 14, 7724-7738.
- [25] Johnson, E. and Becke, A. D. *Can. J. Chem.* 2009, 87, 1369-1373.
- [26] Balcells, D. and Skjelstad, B. B. *J. Chem. Inf. Model.* 2020, 60(12), 6135-6146.
- [27] Hanwell, M. D. *J. Chem. Inf.* 2012, 4(17), 1-17.
- [28] O'Boyle, N. M. *J. Chem. Inf.* 2011, 3(33), 1-14.
- [29] Neese, F. (2012) *Wiley Interdiscip. Rev.: Comput. Mol. Sci.* 2012, 2, 73-78.
- [30] Neese, F. (2017) *Wiley Interdiscip. Rev.: Comput. Mol. Sci.* 2017, 8, e1327.